ID-Blau: Image Deblurring by Implicit Diffusion-based reBLurring AUgmentation

Supplementary Material

In the supplementary material, we also compared other augmentation methods, and the results showed that our ID-Blau method outperforms them. Additionally, We provide additional reblurred results by ID-Blau to demonstrate ID-Blau's ability to generate realistic reblurred images. Besides, we demonstrate deblurring results with and without using ID-Blau on RWBI [10], which contains real-world blurred images without ground truth.

1. Comparison with other augmentation methods.

BSDNet [5] disentangles content and blur features for reblurring. However, BSDNet cannot pixel-wisely or arbitrarily control blur patterns compared to ID-Blau. Since BSDNet has not released the code, we compare the performance reported in its paper. Table 1 shows the reblurring performance on the GoPro test set (also see Table IV in BSDNet). The results demonstrate that ID-Blau can regenerate blur patterns more precisely than BSDNet. SBDD [1] utilizes predefined blur kernels to convolve sharp images for reblurring. However, since blur patterns are usually unknown during testing, using predefined kernels, in general, is suboptimal. Table 2 compares the performances of ID-Blau and SBDD under the same training strategy as ID-Blau, and demonstrates that ID-Blau outperforms SBDD.

Table 1. Comparison of reblurring performance among BGAN, BSDNet, and ID-Blau on GoPro test set. All methods are trained on GoPro training set.

Model	PSNR ↑	SSIM ↑	LPIPS ↓
BGAN	26.28	0.906	0.213
BSDNet	32.09	–	–
ID-Blau	**32.91**	**0.960**	**0.079**

Table 2. Comparison of deblurring performance among SBDD and ID-Blau on the GoPro test set. We use the same strategy, *i.e.* pre-training followed by fine-tuning, for all methods.

Model	Baseline	+SBDD	+ID-Blau
MIMO-UNet (PSNR ↑)	31.22	31.47	**32.02**

2. Reblurred Visualizations Results of ID-Blau

Reblurring through optical flows. We show additional visualizations to emphasize ID-Blau's ability to generate high-quality blurred images with various conditions. In Figure 1, 2, and 3, we use a sharp image S and a blur condition map $C = [x; y; z]$ from the GoPro training set [6] as the inputs to generate the corresponding blurred image. Moreover, in each figure, we generate four more blur condition maps based on C for further illustration, including horizontal and vertical blur orientations, $C^1 = [1; 0; z]$ and $C^2 = [0; 1; z]$, horizontally reversed C as $C^3 = [-x; y; z]$, and $C^4 = [-x; y; 2z]$, which magnifies blur magnitudes of C^3 by twice. These visualizations demonstrate ID-Blau's ability to generate diverse blurred images.

Reblurring through semantic segmentation maps. To verify the generalization ability of ID-Blau on unseen sharp images, we apply ID-Blau to the PASCAL VOC 2012 [3] dataset, which provides sharp images with semantic segmentation maps. The semantic segmentation maps provide the object-level location for each pixel, allowing us to convert them to blur condition maps for ID-Blau. Therefore, we can utilize sharp images in the PASCAL VOC 2012 dataset with various blur condition maps generated for producing diverse blurred images using ID-Blau. Figure 4 shows some generated blurred examples from the PASCAL dataset using ID-Bau trained on the GoPro training set. These results verify ID-Blau's robustness in generating high-quality blurred images from unseen sharp images. Furthermore, as can be seen in the figure 5, we specify different blur conditions on the left and right sides of a map to generate inharmonious blurred images. Despite using inharmonious blur condition maps, ID-Blau can still generate blur at pixel-level precision, demonstrating ID-Blau's stability for generating blurry images.

3. Deblurring Results on Real-World Blurry Images

We provide additional qualitative comparisons among deblurring models (deblurring baselines, denoted "Baseline" and their ID-Blau-powered versions, denoted "ID-Blau") trained on RealBlur-J [7] and tested on RWBI [10] dataset. The RWBI dataset contains real-world blurred images without ground truth. We demonstrate the qualitative comparisons of MIMO-UNet+ [2] in Figures 6 and 7, Restormer [9] in Figures 8 and 9, Stripformer [8] in Figures 10 and 11, and FFTformer [4] in Figures 12 and 13. The qualitative results demonstrate ID-Blau's ability to improve deblurring results on real-world blurry images.

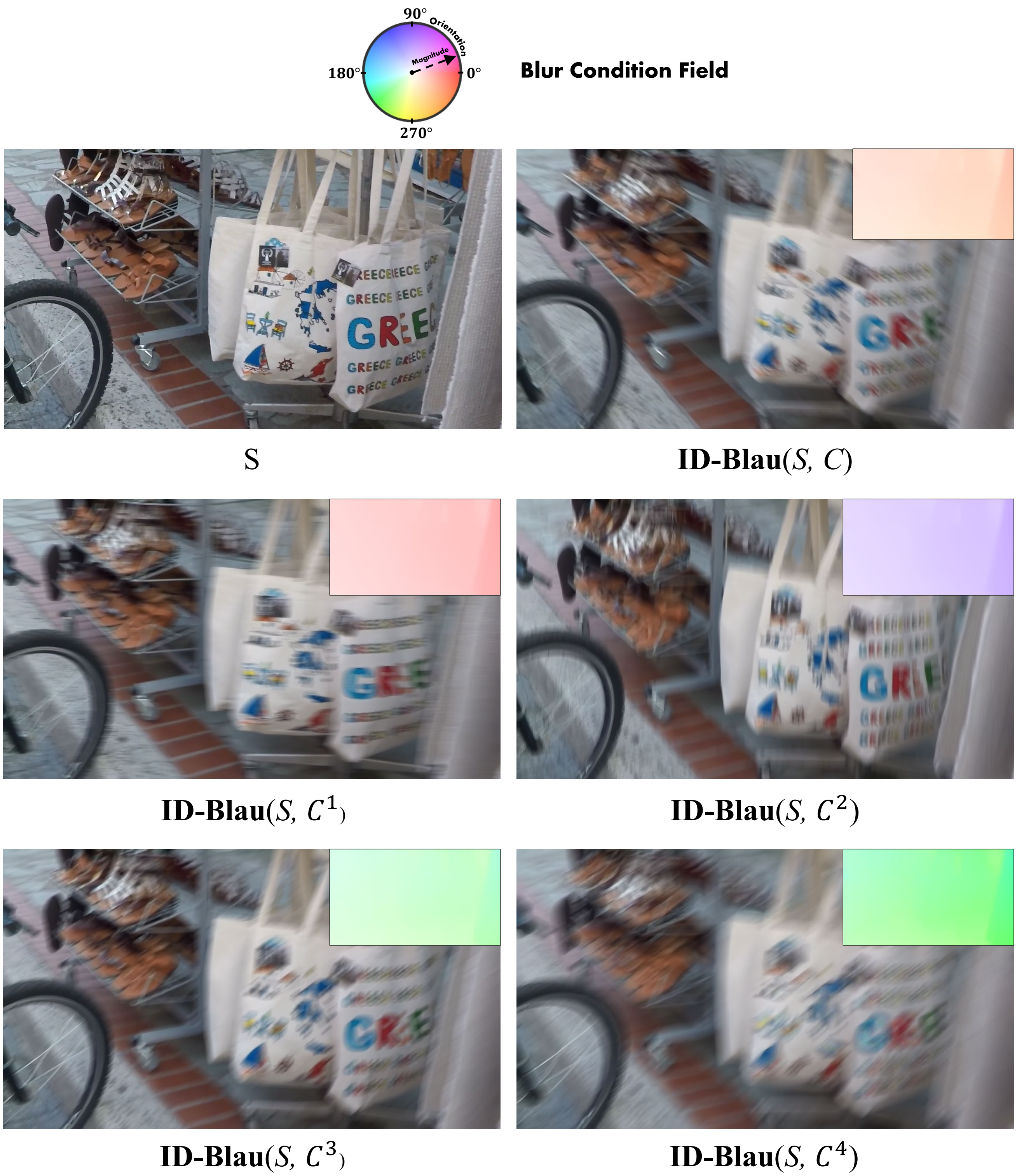

Figure 1. Qualitative reblurred results of ID-Blau on the GoPro training set [6].

Figure 2. Qualitative reblurred results of ID-Blau on the GoPro training set [6].

Figure 3. Qualitative reblurred results of ID-Blau on the GoPro training set [6].

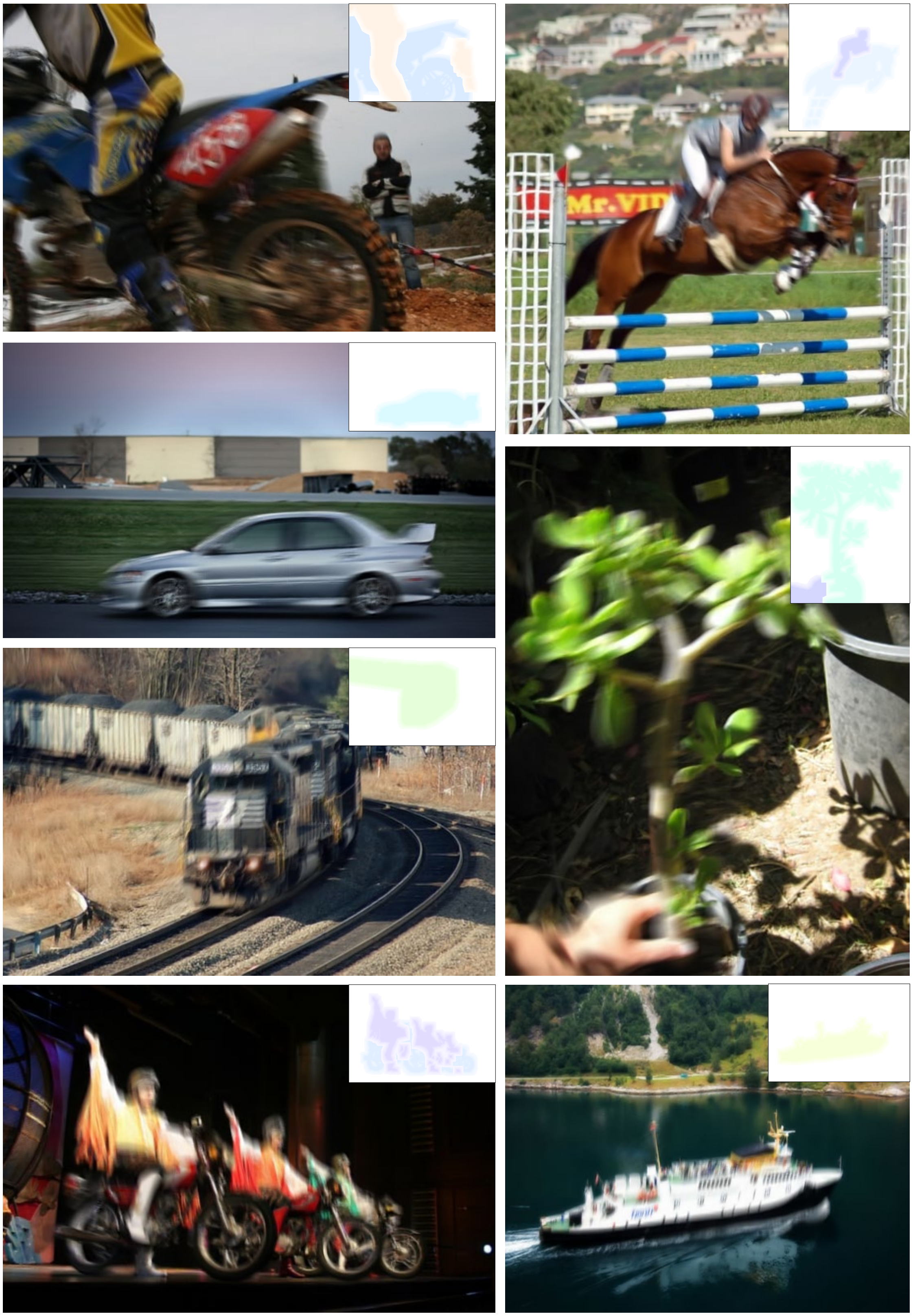

Figure 4. Qualitative reblurred results of ID-Blau on the PASCAL VOC 2012 [3] dataset. We used sharp images and altered blur conditions to generate various blurred images.

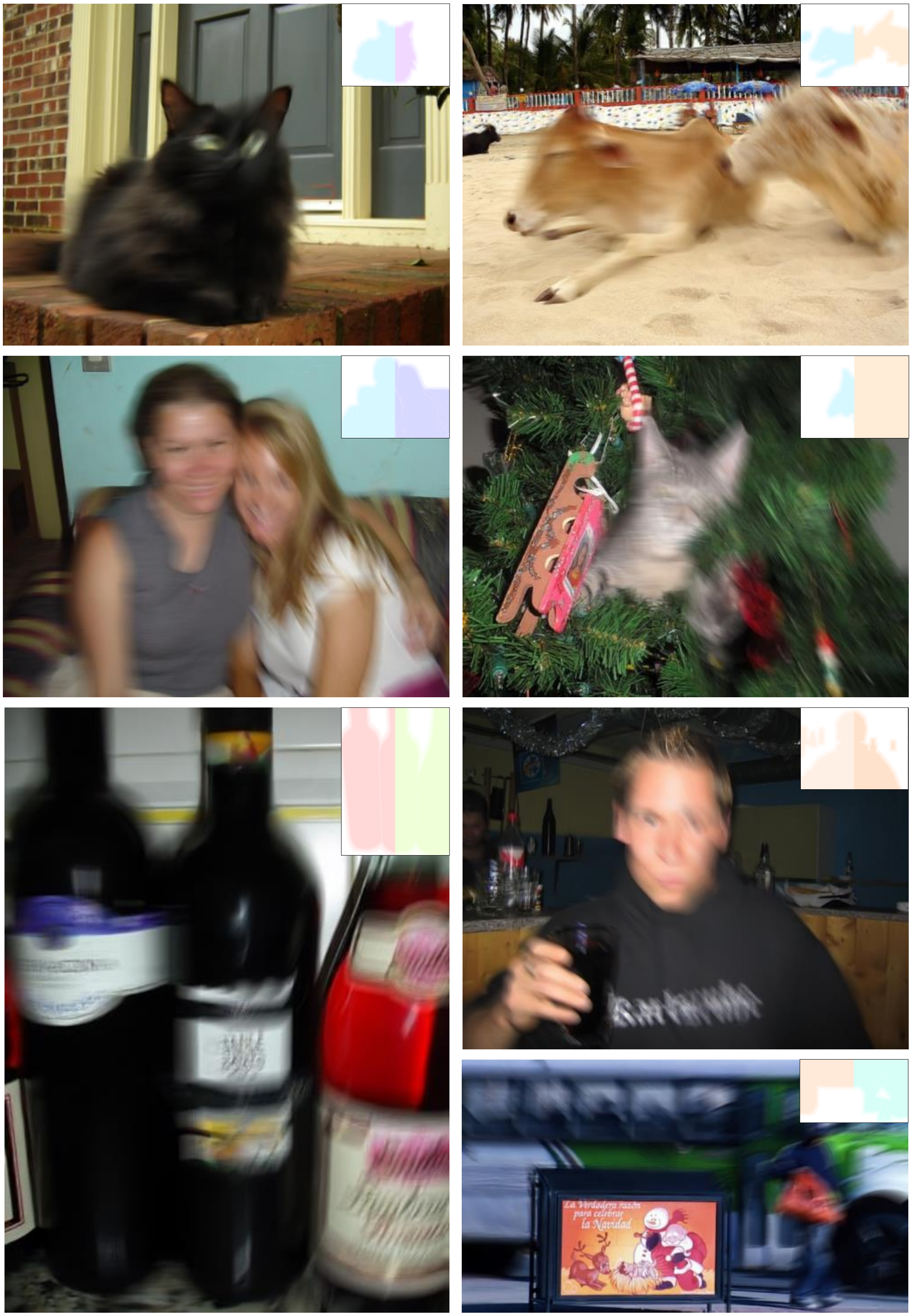

Figure 5. Qualitative reblurred results of ID-Blau on the PASCAL VOC 2012 [3] dataset. We utilized sharp images and intentionally deviated blur conditions to generate blurred images.

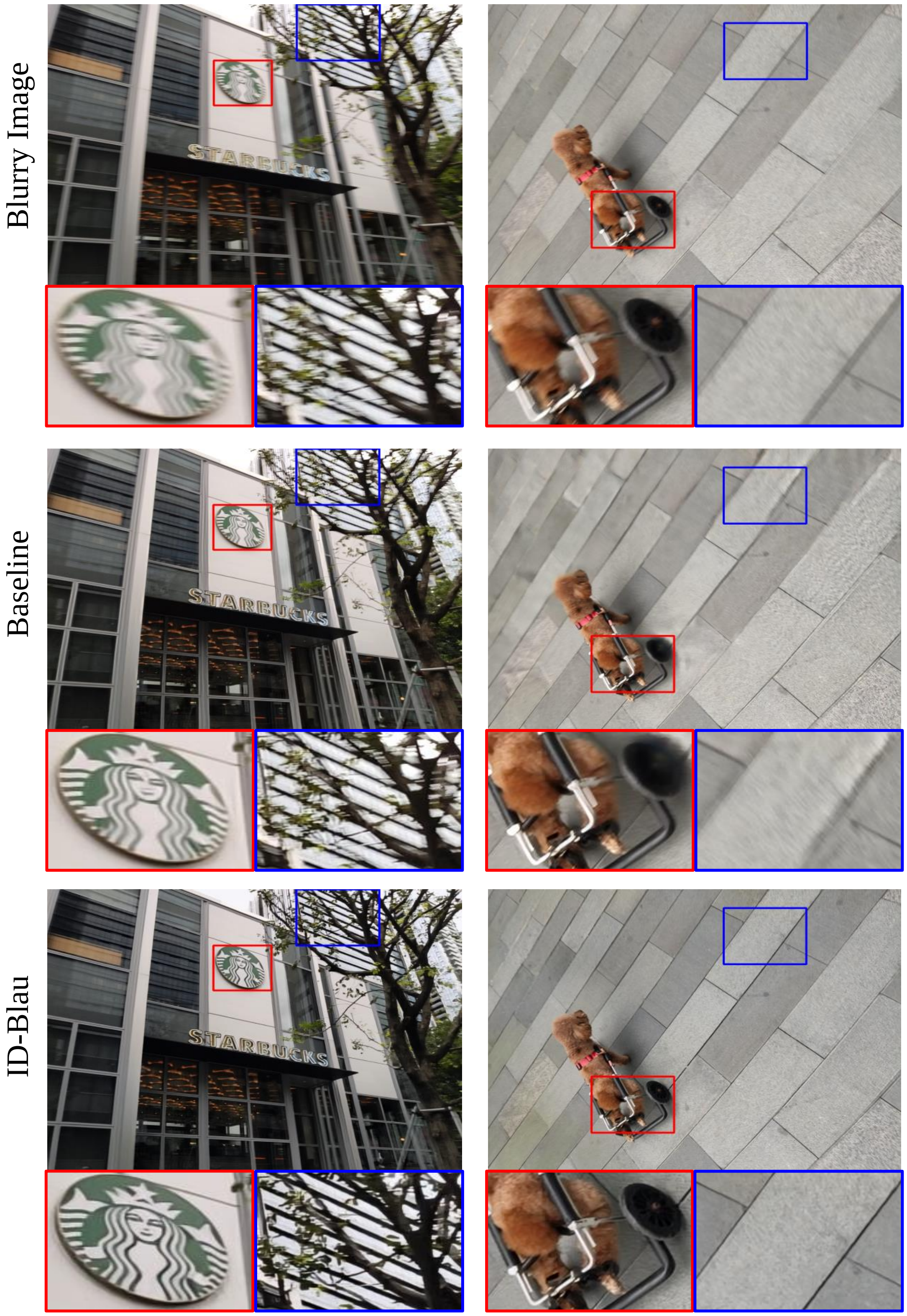

Figure 6. Qualitative results of MIMO-UNet+ [2] on the RWBI [10] dataset.

Figure 7. Qualitative results of MIMO-UNet+ [2] on the RWBI [10] dataset.

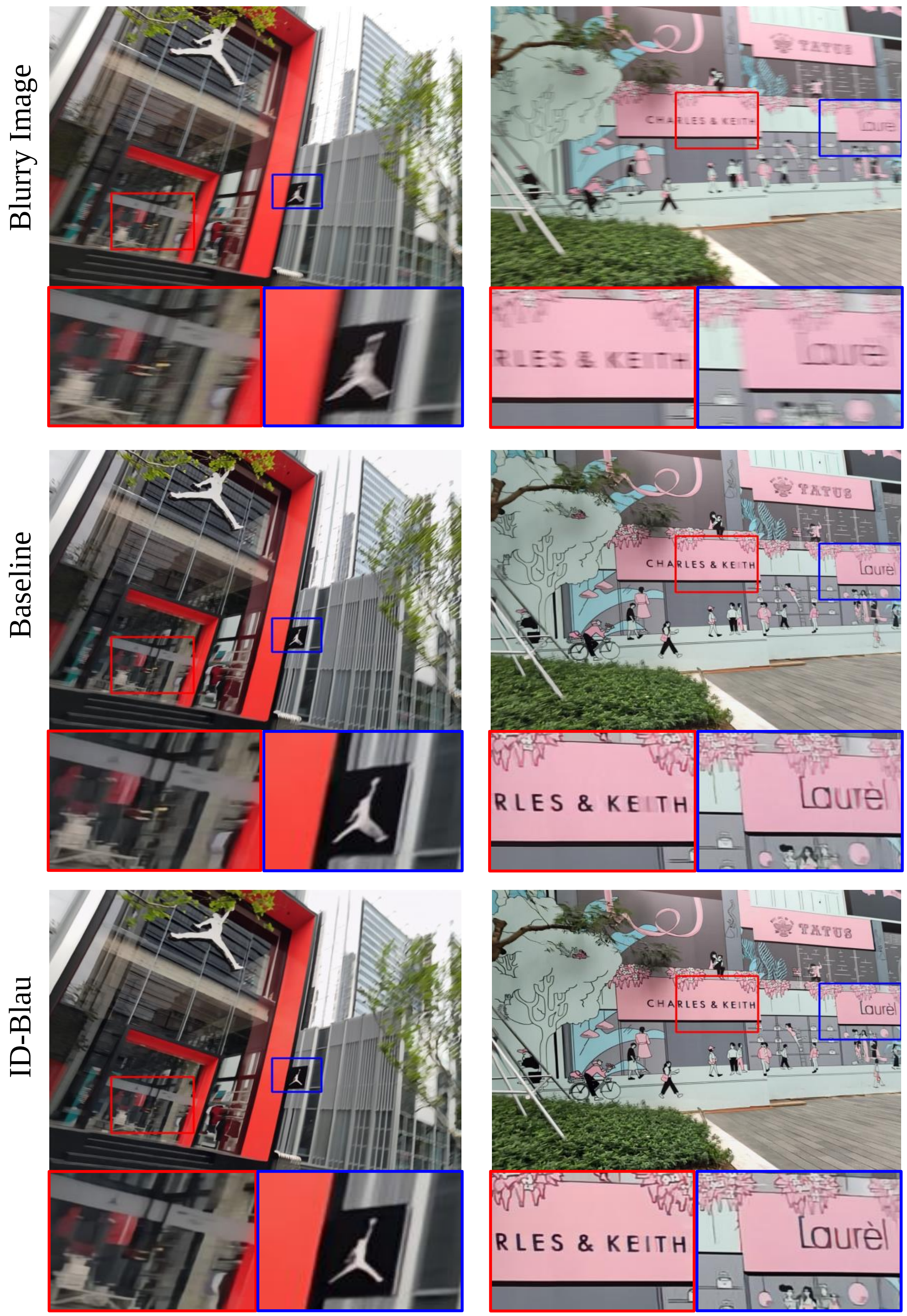

Figure 8. Qualitative results of Restormer [9] on the RWBI [10] dataset.

Figure 9. Qualitative results of Restormer [9] on the RWBI [10] dataset.

Figure 10. Qualitative results of Stripformer [8] on the RWBI [10] dataset.

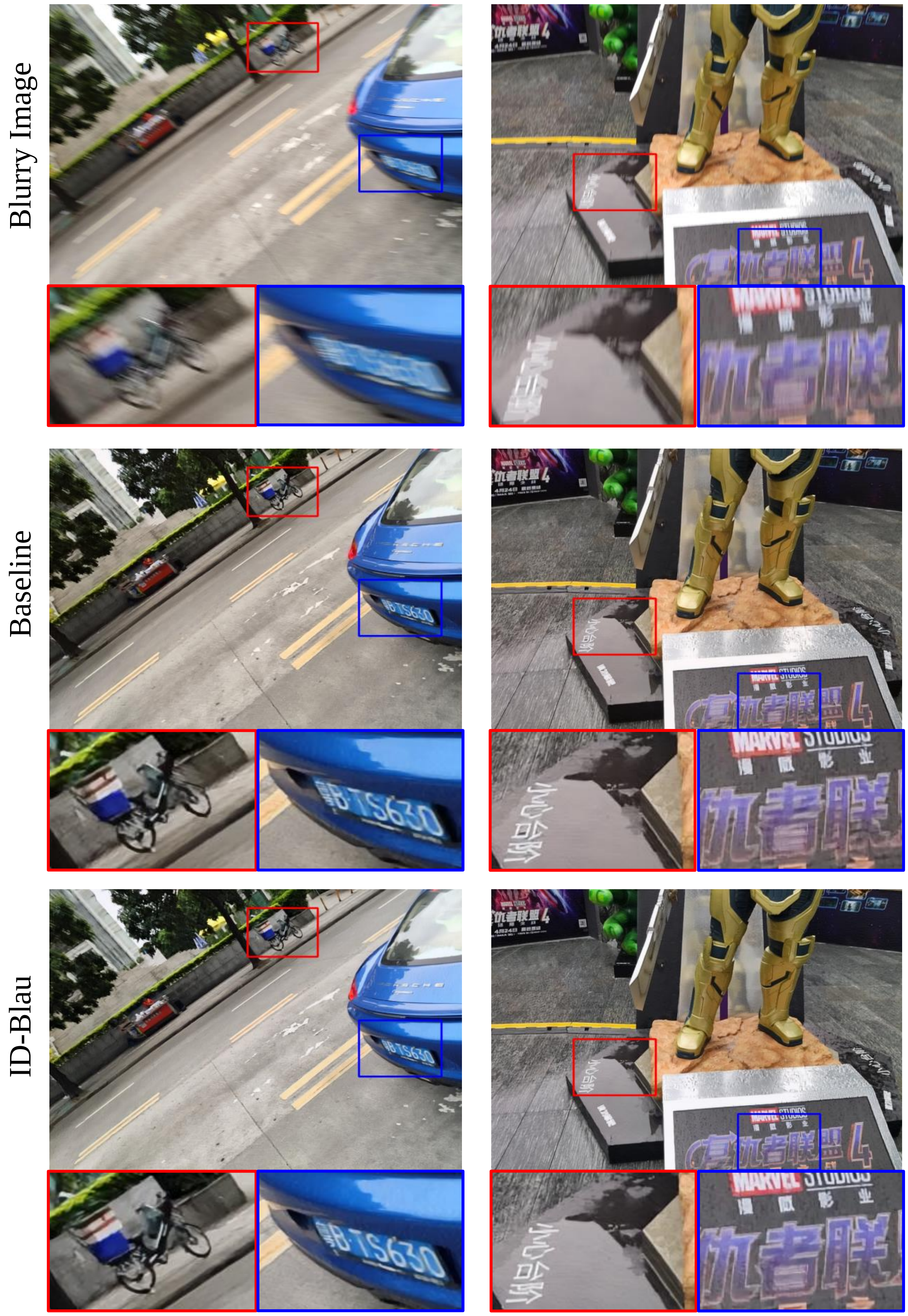

Figure 11. Qualitative results of Stripformer [8] on the RWBI [10] dataset.

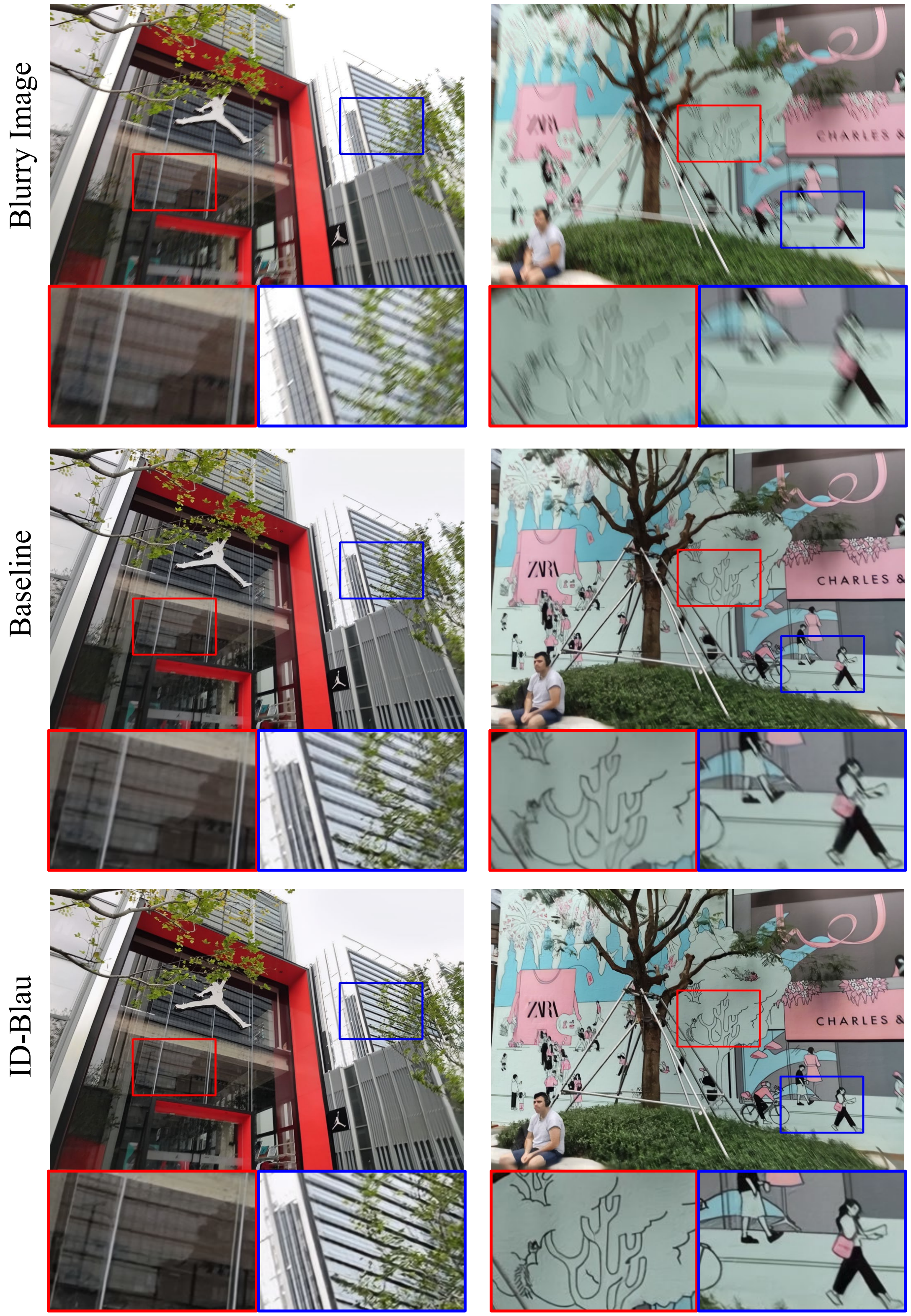

Figure 12. Qualitative results of FFTformer [4] on the RWBI [10] dataset.

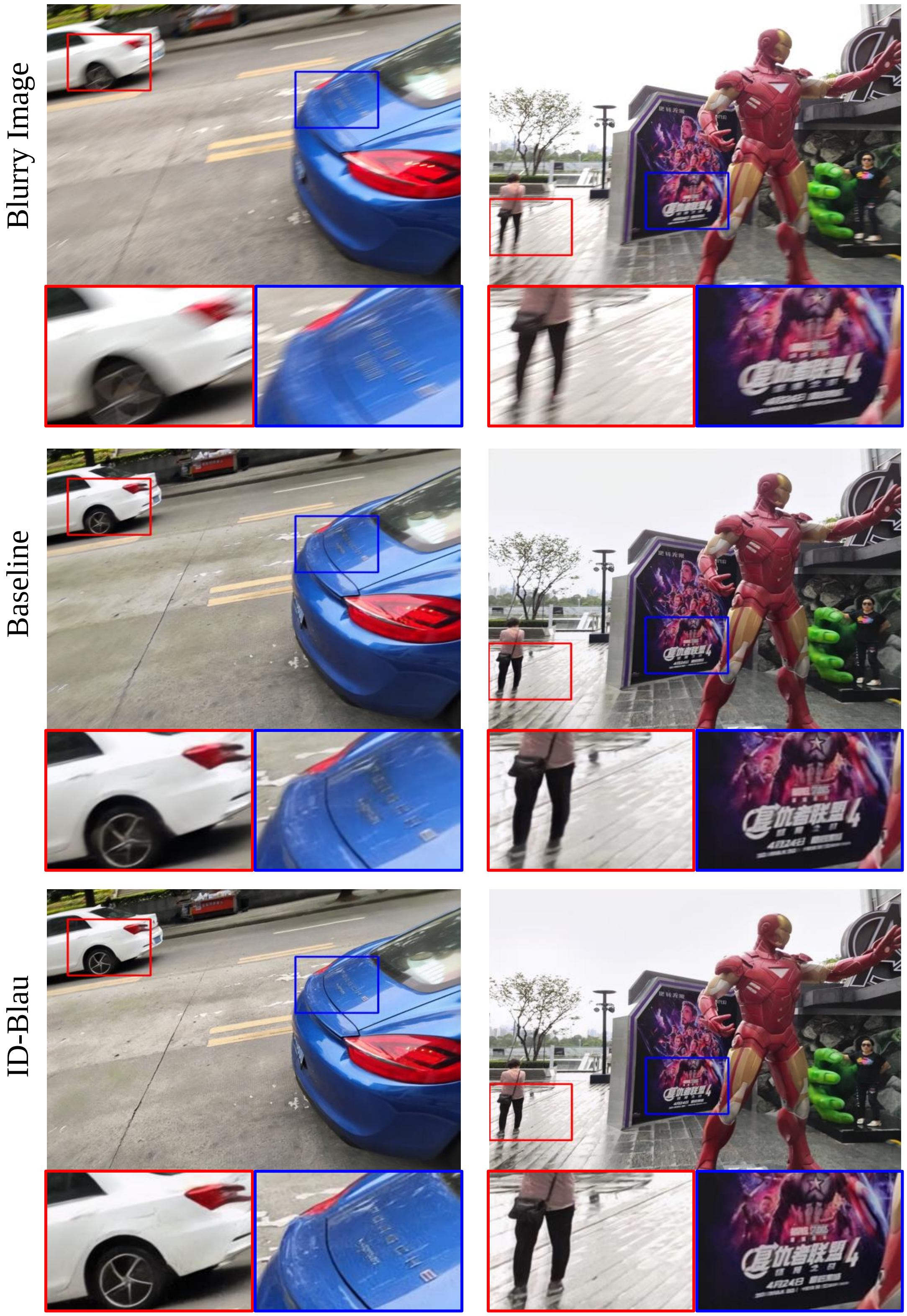

Figure 13. Qualitative results of FFTformer [4] on the RWBI [10] dataset.

References

[1] Guillermo Carbajal, Patricia Vitoria, Pablo Musé, and José Lezama. Improving generalization of deep motion deblurring networks: A convolution-based procedure for analyzing and addressing the limitations of current benchmark datasets. In *SSRN*, 2023. 1

[2] Sung-Jin Cho, Seo-Won Ji, Jun-Pyo Hong, Seung-Won Jung, and Sung-Jea Ko. Rethinking coarse-to-fine approach in single image deblurring. In *ICCV*, 2021. 1, 7, 8

[3] M. Everingham, L. Van Gool, C. K. I. Williams, J. Winn, and A. Zisserman. The PASCAL Visual Object Classes Challenge 2012 (VOC2012) Results. 1, 5, 6

[4] Lingshun Kong, Jiangxin Dong, Jianjun Ge, Mingqiang Li, and Jinshan Pan. Efficient frequency domain-based transformers for high-quality image deblurring. In *CVPR*, 2023. 1, 13, 14

[5] Ziyao Li, Zhi Gao, Han Yi, Yu Fu, and Boan Chen. Image deblurring with image blurring. In *IEEE TIP*, 2023. 1

[6] Seungjun Nah, Tae Hyun Kim, and Kyoung Mu Lee. Deep multi-scale convolutional neural network for dynamic scene deblurring. In *CVPR*, 2017. 1, 2, 3, 4

[7] Jaesung Rim, Haeyun Lee, Jucheol Won, and Sunghyun Cho. Real-world blur dataset for learning and benchmarking deblurring algorithms. In *ECCV*, 2020. 1

[8] Fu-Jen Tsai, Yan-Tsung Peng, Yen-Yu Lin, Chung-Chi Tsai, and Chia-Wen Lin. Stripformer: Strip transformer for fast image deblurring. In *ECCV*, 2022. 1, 11, 12

[9] Syed Waqas Zamir, Aditya Arora, Salman Khan, Munawar Hayat, Fahad Shahbaz Khan, and Ming-Hsuan Yang. Restormer: Efficient transformer for high-resolution image restoration. In *CVPR*, 2022. 1, 9, 10

[10] Kaihao Zhang, Wenhan Luo, Yiran Zhong, Lin Ma, Bjorn Stenger, Wei Liu, and Hongdong Li. Deblurring by realistic blurring. In *CVPR*, 2020. 1, 7, 8, 9, 10, 11, 12, 13, 14